4. Bürgmann, R., Kogan, M., Levin, V., Scholz, C., King, R. and Steblov, G., Rapid aseismic moment release following the 5 December 1997 Kronotsky, Kamchatka earthquake. *Geophys. Res. Lett.*, 2001, **28**, 1331–1334.
5. Heki, K., Miyazaki, S. and Tsuji, H., Silent fault slip following an interplate thrust earthquake at the Japan Trench. *Nature*, 1997, **386**, 595–598.
6. Melbourne, T. I., Webb, F. H., Stock, J. M. and Reigber, C., Rapid postseismic transients in subduction zones from continuous GPS. *J. Geophys. Res. B*, 2002, **107**, 2241.
7. Dragert, H., Wang, K. and James, T., A silent slip event on the deeper Cascadia subduction interface. *Science*, 2001, **292**, 1525–1528.
8. Miller, M. M., Melbourne, T., Johnson, D. J. and Sumner, W. Q., Periodic slow earthquakes from the Cascadia Subduction Zone. *Science*, 2002, **295**, 2423.
9. Rogers, G. and Dragert, H., Episodic tremor and slip on the Cascadia Subduction Zone: The chatter of silent slip. *Science*, 2003, **300**, 1942–1944.
10. Szeliga, W., Melbourne, T. I., Miller, M. M. and Santillan, V. M., Southern Cascadia episodic slow earthquakes. *Geophys. Res. Lett.*, 2004, **31**, L16602.
11. Melbourne, T. I. and Webb, F. H., Slow but not quite silent. *Science*, 2003, **300**, 1886–1887.
12. Stein, S. and Okal, E. A., Speed and size of the Sumatra earthquake. *Nature*, 2005, **434**, 581–582.
13. Ammon, C. J. *et al.*, Rupture process of the 2004 Sumatra–Andaman earthquake. *Science*, 2005, **308**, 1133–1139.
14. Lay, T. *et al.*, The Great Sumatra–Andaman earthquake of 26 December 2004. *Science*, 2005, **308**, 1127–1133.
15. Catherine, J. K., Gahalaut, V. K. and Sahu, V. K., Constraints on rupture of the December 26, 2004, Sumatra earthquake from far-field GPS observations. *Earth Planet. Sci. Lett.*, 2005, **237**, 673–679.
16. Banerjee, P., Pollitz, F. F. and Bürgmann, R., The size and duration of the Sumatra–Andaman earthquakes from far-field static offsets. *Science*, 2005, **308**, 1769–1772.
17. Jade, S., Vijayan, M. S. M., Gupta, S. S., Dileep Kumar, P., Gaur, V. K. and Arumugam, S., Effect of *M* 9.3 Sumatra–Andaman Islands earthquake of 26th December 2004 at some permanent and campaign GPS stations in the Indian continent. *Int. J. Remote Sensing* (in press).
18. Kreemer, C., Blewitt, G., Hammond, W. C. and Plag, H.-P., Global deformation from the great 2004 Sumatra–Andaman earthquake observed by GPS: Implications for rupture process and global reference frame. *Earth Planet. Space*, 2006, **58**, 141–148.
19. King, R. and Bock, Y., Documentation for the GAMIT GPS Analysis Software, Release 9.94. Mass. Inst. of Technol., Cambridge, Mass., and Scripps Inst. of Oceanogr., La Jolla, Calif., 2000.
20. Herring, T., Global Kalman Filter VLBI and GPS Analysis Program (GLOBK), version 5.0. Mass. Inst. of Technol., Cambridge, Mass, 2000.
21. Kreemer, C., Holt, W. E. and Haines, A. J., An integrated global model of present day plate motions and plate boundary deformation. *Geophys. J. Int.*, 2003, **154**, 8–34.
22. Gahalaut, V. K., Nagarajan, B., Catherine, J. K. and Kumar, S., Constraints on 2004 Sumatra–Andaman earthquake rupture from GPS measurements in Andaman–Nicobar Islands. *Earth Planet. Sci. Lett.*, 2006, **242**, 365–374.
23. Jade, S., Ananda, M. B., Dileep Kumar, S. P. and Banerjee, S., Coseismic and postseismic displacements in Andaman and Nicobar Islands from GPS measurements. *Curr. Sci.*, 2005, **88**, 1980–1984.
24. Earnest, A., Rajendran, C. P., Rajendran, K., Anu, R., Arun, G. M. and Mohan, P. M., Near-field observations on the co-seismic deformation associated with the 26 December 2004 Andaman–Sumatra earthquake. *Curr. Sci.*, 2005, **89**, 1237–1244.
25. Subarya, C. *et al.*, Plate-boundary deformation associated with the great Sumatra–Andaman earthquake. *Nature*, 2006, **440**, 46–51.
26. Gahalaut, V. K. and Catherine, J. K., Rupture characteristics of 28 March 2005 Sumatra earthquake from GPS measurements and its implication for tsunami generation. *Earth Planet. Sci. Lett.*, 2006, **249**, 39–46.
27. Briggs, R. W. *et al.*, Deformation and slip along the Sunda megathrust in the Great 2005 Nias-Simeulue earthquake. *Science*, 2006, **311**, 1897–1901.
28. Bourgeois, J., A movement in four parts? *Nature*, 2006, **440**, 430–431.
29. Scholz, C., Earthquakes and friction laws. *Nature*, 1998, **391**, 37–42.
30. Curray, J. R., Tectonics and history of the Andaman sea region. *J. Asian Earth Sci.*, 2005, **25**, 187–228.
31. Paul, J. *et al.*, The motion and active deformation of India. *Geophys. Res. Lett.*, 2001, **28**, 647–650.
32. Banerjee, P., Pollitz, F., Nagarajan, B. and Bürgmann, R., Coseismic slip distributions of the 26 December 2004 Sumatra–Andaman and 28 March 2005 Nias earthquakes from GPS static offsets. *Bull. Seismol. Soc. Am.*, 2006 (in press).

ACKNOWLEDGEMENTS. We thank Dr J. R. Kayal, GSI, Kolkata for his in-depth and constructive review, which helped improved the MS. We also thank the Director, NGRI, Hyderabad and Dr R. K. Chadha, NGRI, Hyderabad, for support and DST for financial support.

Received 10 April 2006; revised accepted 7 August 2006

Discovery of volcanic ash bed from the basal Subathu Formation (Late Palaeocene–Middle Eocene) near Kalka, Solan District (Himachal Pradesh), Northwest Sub-Himalaya, India

N. Siva Siddaiah* and Kishor Kumar

Wadia Institute of Himalayan Geology,
33, General Mahadeo Singh Road, Dehradun 248 001, India

Discovery of 1.5 m thick volcanic ash bed is reported from the basal part of the Late Palaeocene–Middle Eocene Subathu Formation exposed along the Koshaliya river near Kalka (Solan District) in the foothills of Himachal Pradesh. The ash bed represents the oldest volcanic ash horizon from this part of the Himalayan Foreland Basin. The ash is fine-grained and consists mostly of kaolinite with trace quantities of glass shards, euhedral and angular β-quartz, sanidine, zircon, biotite and anatase. It has high concentrations of Al_2O_3 as well as incompatible elements (Zr, Nb, Th and Y), and high loss on ignition. Based on lithological as-

*For correspondence. (e-mail: nssiddaiah@rediffmail.com)

sociation, field characters, mineralogy and geochemistry, the ash bed has been identified as tonsteins of a volcanic origin. The stratigraphic position and thickness of the ash bed indicate a significant volcanic event during the Early Eocene.

Keywords: Eocene, Himalayan Foreland Basin, Subathu Formation, volcanic ash.

INDIA–Asia collision was responsible for the formation of the Himalaya and uplift of the Tibetan Plateau, and is considered to have brought geological, geochemical, climatic and biotic changes of regional to global scale[1–4]. Most geodynamic models suggest that the Indian plate came in contact with the Asian plate sometime during the Palaeocene–Middle Eocene[5–16]. Thus, the age of initiation of this collision remains poorly constrained. Improved understanding of collision timing as well as stratigraphic evidence for the same are crucial for correlation of globally significant events such as volcanism, tectonism, sea-level changes, biotic changes, chemical changes in ocean-water composition, and changes in physical oceanographic pattern. The birth and tectono-sedimentary evolution of the Himalayan Foreland Basin (HFB), which comprises thick succession of marine to continental beds, are directly linked with the collision event and its sediments are excellent proxy records of collisional history and the Tethyan withdrawal. The Late Palaeocene–Middle Eocene Subathu succession that represents the nascent phase of the foreland basin in the northwestern sub-Himalaya has preserved distinct episodes of withdrawal of the Tethys Sea during the India–Asia convergence and the onset of continental setting. It is considered to hold the key for constraining the event and has therefore, attained great importance in recent years.

While pursuing high-resolution systematic studies on older succession of the HFB, we recently discovered a prominent bed of volcanic ash from the basal part of the Subathu Formation exposed along the Koshaliya river in the vicinity of Kalka town (Figure 1). This find has multifold significance, namely (i) this is the first ash bed discovered from the marine part of the Subathu Formation and the oldest from the HFB; (ii) its stratigraphic position corresponds well with the India–Asia collision event and thus is significant for its better understanding; (iii) it has an application in basin wide stratigraphic correlation; (iv) it is a good proxy to understand the nature of volcanism, and (v) it has a direct bearing on the Kakara–Subathu stratigraphic boundary and eventually the Palaeocene–Eocene boundary in the northwest sub-Himalaya. Since, this is the only volcanic ash bed found so far in the lower Subathu Formation, we name it as 'Basal Subathu Tonstein' (BST) for facilitating stratigraphic correlation between geographic regions. Tonsteins are kaolinite-dominated, highly altered volcanic ash beds that occur associated with coal seams[17–19]. The occurrence of 1.5 m thick ash bed at the base of the Subathu Formation indicates an event of significant volcanic activity during the Early Eocene period. The aim of this communication is to describe the stratigraphic position, geographic occurrence, mineralogy and geochemistry of the BST, and highlight its tectonomagmatic and stratigraphic significance vis-à-vis India–Asia collision.

The Subathu succession comprising the oldest beds of the HFB occurs in the NW sub-Himalaya generally overlying the Precambrian sequence[20,21]. It is dominantly marine and consists mainly of grey, green and red shale intercalated with fossiliferous limestone/marl, calcareous siltstone and sandstone. Based on palaeontological evidences the Subathu succession is considered to be of Late Palaeocene (Thanetian) to early Middle Eocene (Lutetian) age[22–29]. The lithological section where we discovered the volcanic ash bed, is exposed along the Koshaliya river in close vicinity of Kalka town, Solan district, Himachal Pradesh. It is approachable by a metalled road that joins the Kalka–Shimla Highway between kilometre stones 64 and 65. In this section, the Subathu sequence overrides the Siwalik succession along Bilaspur Thrust. The base of the Subathu sequence consists of unfossiliferous carbonaceous shales, whereas its topmost part comprises nummulitic green shales directly underlying the quartzose sandstone marking the base of the Dagshai Formation. The location of this section falls in the Survey of India 1 : 50,000 topographic sheet no 53 B/13.

In Figure 2, we have depicted the lithological log of the lower part of the section to show stratigraphic level of the BST with respect to exposed base of the Subathu Formation. The base is marked by two conspicuous coal seams separated by a 1.5 m thick volcanic ash bed that lies 2 to 3 m above the Bilaspur Thrust (Figures 2 and 3). The older coal seam is 2 m thick, while the younger one is only a metre thick. The strike direction of beds in the section ranges between N 10° and 40°W and the dip amount is generally high (> 65°), though the ash bed (BST) appears low-dipping because of disturbance owing to its close proximity with the Bilaspur Thrust (Figure 3).

The newly discovered volcanic ash bed is 1.5 m thick, and occurs sandwiched between the two coal seams in the basal part of the Subathu Formation. It is exposed on the northern as well as southern banks of the Koshaliya river and its strike persistence is ~ 75 m. It has sharp contacts with the underlying and overlying coal seams (Figure 3). The lower 10–25 cm part of the ash bed shows fine streaks of carbonaceous matter. The ash deposit is lightly welded, poorly sorted and massive (Figure 4 *a*). However, presence of lithic/lapilli fragments in the ash bed is not uncommon (Figure 4 *b*). BST is non-calcareous and can be easily pulverized with fingers. It is light grey (2.5 Y, 5/1) to dark grey (2.5 Y, 4/1), soft and soapy, and very fine to medium fine-grained. Its clay-rich nature and physical properties, particularly the light grey colour against black coal horizons makes this ash bed conspicuous, differentiating it from the adjacent beds in the section.

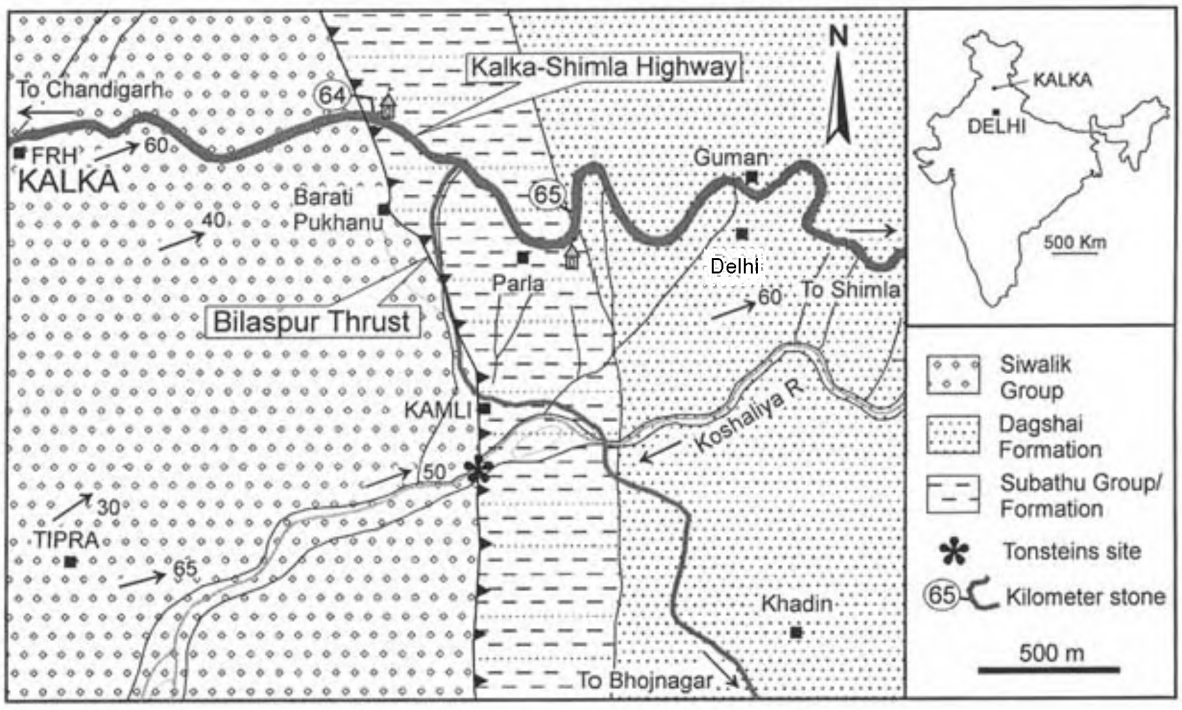

Figure 1. Geological and location map of the area around Kalka showing the Koshaliya river course and the site of Basal Subathu Tonstein (BST).

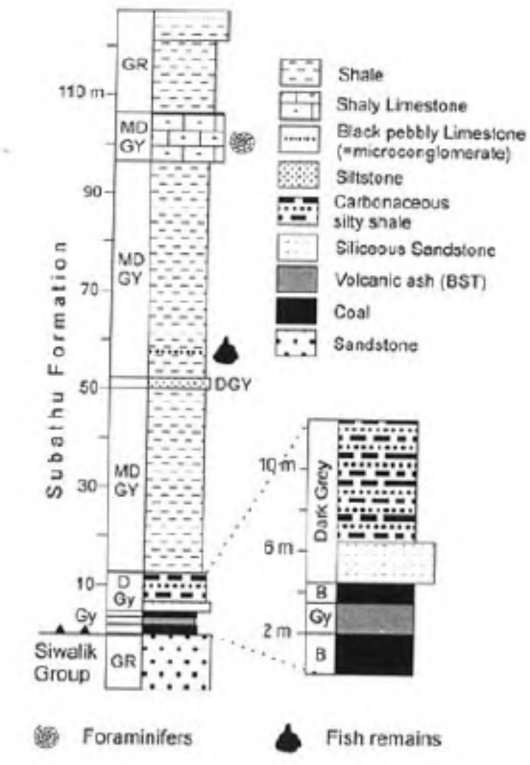

Figure 2. Lithological log of lower part of Subathu Formation exposed along Koshaliya river near Kalka showing stratigraphic position of BST and bounding coal seams. B = black, GY = grey, MDGY = medium grey, DGY = dark grey, and GR = green.

Bulk samples of the volcanic ash bed were collected from freshly cleared exposures. Representative sub-samples were used in making thin sections for petrographic study. Since the ash bed is lightly welded and consists predominantly of fine-grained clay, dry method was followed for preparing its thin sections. For X-ray diffraction (XRD) studies, sample powders were suspended in acetone and air-dried on a clean glass slide. All XRD analyses were performed with CuK_α radiation with an angular range from 2 to 70° 2θ. Representative parts of samples were hand-crushed in a clean and clear polythene bag followed by manual powdering in an agate mortar to –200 mesh. Samples were analysed for major and trace elements by X-ray fluorescence (XRF) spectrometry using pressed powder samples and the data are presented in Table 1. Loss on ignition (LOI) on bulk sample powders was conducted at 950°C. Matrix-matched USGS Reference Standards were used during the analysis and the precision of major and trace element analyses is better than 5%.

Petrographic and XRD studies show that the BST consists predominantly (~95 volume %) of fine-grained kaolinite and only a small amount of non-clay fraction. Kaolinite is distributed uniformly in the vertical profile of the ash bed. The observed sharp XRD reflections at 7.2 and 3.59 Å suggest that kaolinite is well-ordered, which is a characteristic for kaolinites of authigenic/volcanogenic nature[30–33].

The non-clay fraction that constitutes approximately 3–4 volume % in the BST is coarser-grained and consists of

glass shards, euhedral as well as broken crystals such as β-quartz paramorphs and quartz splinters, sanidine, biotite, anatase and pyrite. Glass shards occur in different size and shape such as Pele's hair and Pele's tears, Y-shaped shards and pumice shards with parallel vesicles (Figure 5). Quartz crystals have geometric straight edges, subangular corners, and highly reflective surfaces (Figure 6). Most of the quartz grains in the BST are broken, angular to subangular, monocrystalline and show straight extinction (Figure 7 *a*). Biotite occurs often preserving more or less perfectly the hexagonal outlines of the cleavage flakes (Figure 7 *b*). Sanidine occurs as splintered grains with parallel cleavage, and rarely as rectangular crystals. Pyrite occurs as cubic crystals and may be of diagenetic origin.

Although the quantity of non-clay fraction is small, it provides critical evidence supporting a volcanic origin for the BST. In addition to distinctive mineralogy and morphological characteristics, the markedly lower content of quartz in the BST than in terrigenous mudstone/shale also suggests a volcanic origin. The predominance of kaolinite in the BST indicates that most of the original ash was glass, as is typical of many tonsteins known elsewhere in the world[34]. Additionally, the uniform distribution of kaolinite in vertical profile of the ash bed excludes weathering-related processes of kaolinite formation.

The major element composition of the BST is relatively uniform (Table 1). It has high concentration of Al_2O_3 (36–40 wt%), high loss on ignition (10–11 wt%), and low concentrations of Na_2O (0.45 wt%) and MgO (0.5 wt%) relative to terrigenous shale/mudstone. Identification of kaolinite as a dominant component of the clay fraction is consistent with high Al_2O_3 concentration. BST also has much higher concentration of incompatible trace elements such as Zr (735 ppm), Nb (45 ppm), Th (69 ppm) and Y (58 ppm) than in terrigenous shale/mudstone. Samples with 550–750 ppm of zirconium are unlikely to have been derived from mudstones/shale, which has an average concentration of only ~ 160 ppm[35].

The low SiO_2/Al_2O_3 ratio (1.2) compared to mudstone/shale (5.0), suggests an argillization of volcanic glass and thus, rules out the possibility of it being a shale. In addition, low contents of MgO (0.36–0.5 wt%) and CaO (0.11–0.14 wt%) are atypical of mudstone for which the average ranges from 2.5 to 3.0 wt% each[35]. The high loss on ignition (11 wt%) is consistent with hydration and accompanying alteration of glass and formation of kaolinite. Similarly, in the absence of detrital quartz, SiO_2/Al_2O_3 ratios are also lower for volcanic clays due to the fact that SiO_2 is lost during glass-to-clay conversion.

Figure 3. Field photographs of basal part of Subathu Formation showing BST and bounding coal seams. ***a***, Panoramic view, ***b***, Enlarged view showing sharp contact of BST with the lower coal seam.

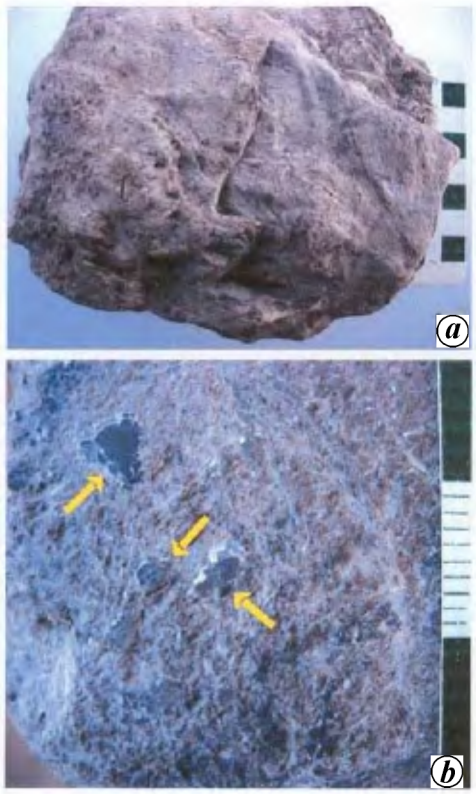

Figure 4. Photographs of hand specimens of BST showing its massive nature (***a***), and lithic fragments indicated by arrows in clay matrix (***b***). Each scale division equals 10 mm in (***a***), and 1 mm in (***b***).

Table 1. Major and trace element content in BST. Comparative data on volcanogenic tonsteins and terrigenous shale (SCo-1) are from the published literature

	Basal Subathu tonsteins			Tonstein[19] (volcanic)	SCo-1[35] (terrigenous)
	1	2	3		
In wt%					
SiO_2	43.41	43.9	44.20	44.1	62.78
Al_2O_3	36.42	37.2	39.16	33.7	13.67
Fe_2O_3	4.02	1.7	0.97	0.70	5.14
MgO	0.50	0.43	0.36	0.27	2.72
CaO	0.14	0.10	0.11	0.17	2.62
Na_2O	0.48	0.45	0.47	0.15	0.9
K_2O	4.48	3.95	3.69	0.41	2.77
TiO_2	1.58	1.6	1.69	1.28	0.62
MnO	0.018	0.01	0.012	0.02	0.052
P_2O_5	0.054	0.05	0.053	0.05	0.206
LOI	10.18	10.2	10.65	19.1	8.8
Total	101.2	99.46	101.3	99.95	100.2
SiO_2/Al_2O_3	1.19	1.18	1.13	1.30	4.59
In parts per million					
Zr	515	605	735	462	160
Y	50.4	50.1	57.6	50	26
Th	59.3	62.3	69.0	48	9.7
Nb	36.7	41.7	44.0	32	11
Ga	54.7	60.0	60.2	44	15
Sc	28	25	24	25	11
U	3.2	3.1	2.9	7	
Rb	203	181	173	19	112
Sr	151	150	148	91	174
Co	9	4	3	2	11
Ni	25.3	27.2	31.6	28	27
Cu	22	26	30.9	19	29
Zn	21.1	20.3	19.3	19	103
Pb	12.1	12.5	14.9		31
Cr	166	179	185	95	68
V	244	267	278	45	131
Ba	454	429	410	299	570

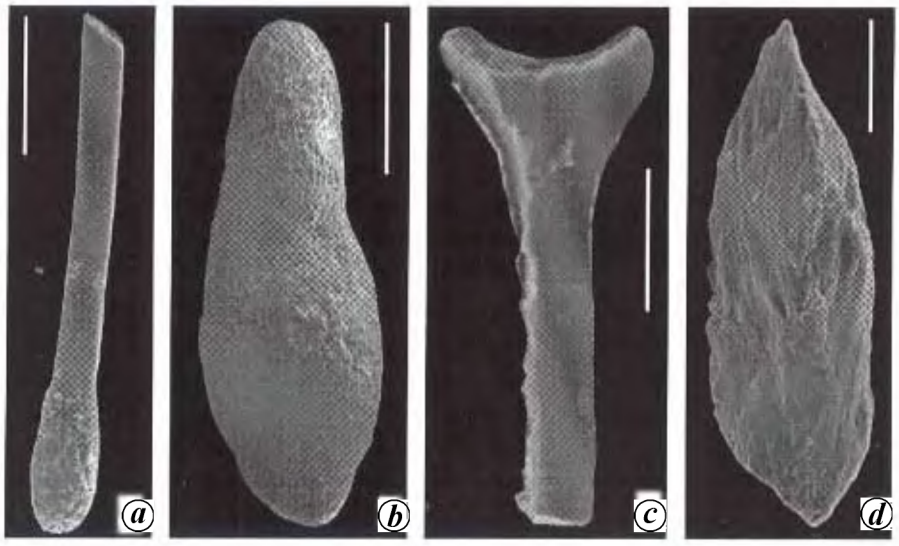

Figure 5. SEM images of glass shards from BST. ***a***, Fragment of Pele's hair with a tear drop; ***b***, Pele's tear; ***c***, Y-shaped shard and ***d***, Shard with elongate vesicles. Scale bars equal 300 μm in (***a***) and (***b***), and 100 μm in (***c***) and (***d***).

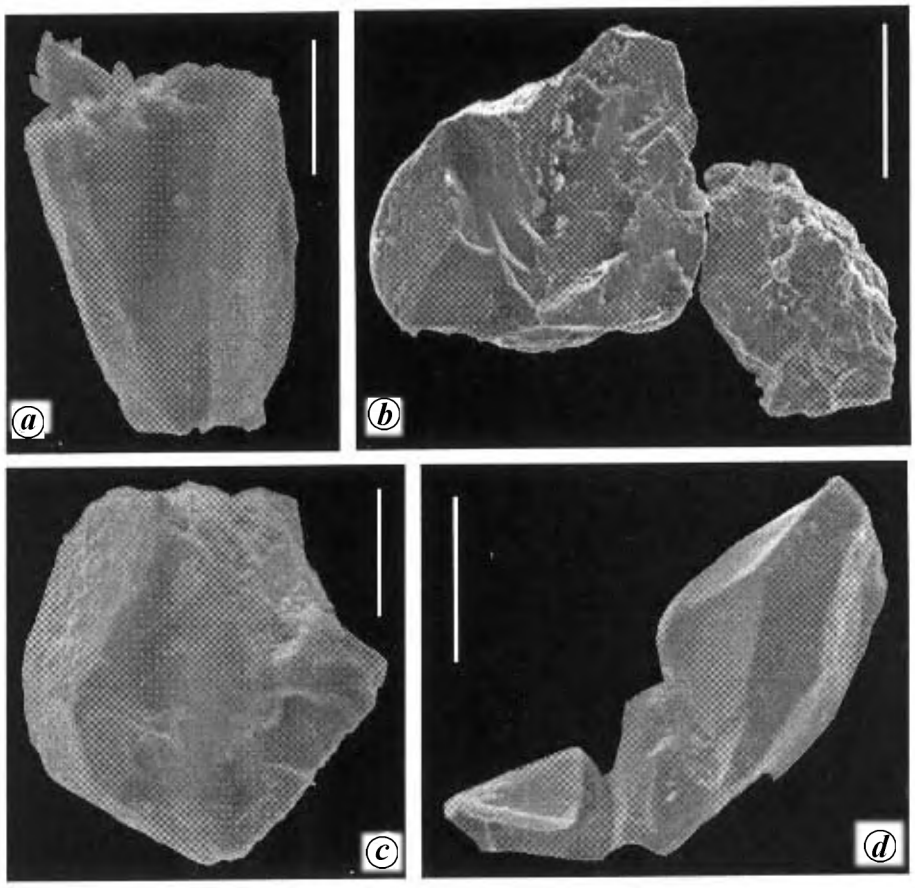

Figure 6. SEM images of euhedral and broken quartz crystals from BST. Scale bars equal 20, 70, 30 and 50 μm in (*a*)–(*d*) respectively.

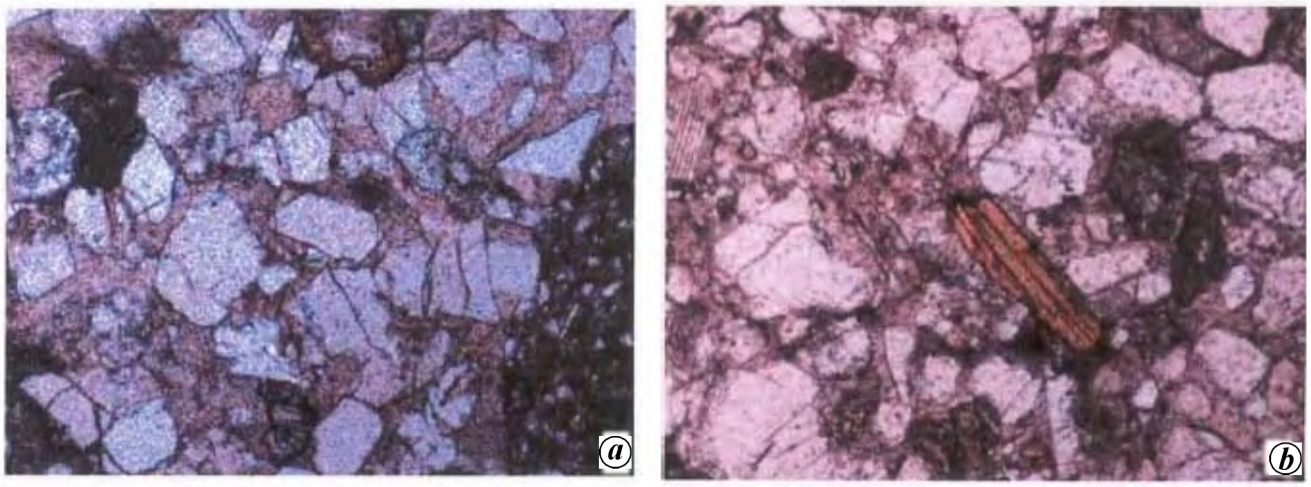

Figure 7. Photomicrographs of thin sections of BST showing clay matrix with euhedral and fractured crystals of quartz in (*a*), and euhedral biotite and quartz (*b*), Plane polarized light, 50X.

The high concentration of Zr (515–735 ppm) indicates the presence of zircon in the BST. The major oxide composition of the BST is consistent with its observed mineralogy and it is similar to that of the volcanogenic tonsteins reported from Europe and North America[36–38]. Major and trace elements data of the Subathu volcanic ash complement the field and petrographic observations and indicate a volcanic origin.

The ash bed discovered in the basal part of the Subathu Formation has field, petrographic, mineralogical and geochemical characteristics analogous to those for volcanogenic tonsteins widely known in Europe and North America[18].

The salient characteristics of the BST by which it can be recognized as altered volcanic ash are: (i) sharp upper and lower contacts; (ii) bimodal grain size distribution, i.e. sand/silt-sized non-clay minerals in a fine clay-sized matrix; (iii) presence of glass shards and lithic fragments; (iv) limited but distinct mineralogical make-up of euhedral or broken volcanic crystals such as β-quartz paramorphs and quartz splinters and high-temperature minerals like sanidine and zircon; (v) nearly monomineralic clay mineral composition (i.e. kaolinite) with sharp XRD peaks, and its uniform vertical distribution in the ash bed; (vi) absence of terrigenous quartz as well as carbonate minerals; (vii) high content of Al_2O_3 (36–40 wt%), high loss on ignition (10–11 wt%), and low concentrations of Na_2O (0.45 wt%), MgO (0.5 wt%) and CaO (0.11–0.14 wt%) and (viii) high concentrations of incompatible trace elements such as Zr. The BST, by virtue of its stratigraphic position and thickness, is important for systematic studies on various aspects, including radiometric dating and petrogenesis to acquire insights into the early phase of the Himalayan orogeny.

1. Garzanti, E., Baud, A. and Mascle, G., Sedimentary record of the northward flight of India and its collision with Eurasia (Ladakh Himalaya, India). *Geodyn. Acta*, 1987, **1**, 297–312.
2. Raymo, M. E. and Ruddiman, W. F., Tectonic forcing of late cenozoic climate. *Nature*, 1992, **359**, 117–122.
3. Edmond, J., Himalayan tectonics, weathering processes, and the strontium isotope record of marine limestones. *Science*, 1992, **258**, 1594–1597.
4. Gunnell, Y., Passive margin uplifts and their influence on climatic change and weathering patterns of tropical shield regions. *Global Planet. Change*, 1998, **18**, 47–57.
5. Molnar, P., England, P. and Martinod, J., Mantle dynamics, the uplift of the Tibetan Plateau, and the Indian monsoon. *Rev. Geophys.*, 1993, **31**, 357–396.
6. Patriat, P. and Achache, J., India–Asia collision chronology has implications for crustal shortening and driving mechanism of plates. *Nature*, 1984, **311**, 615–621.
7. Searle, M. P. *et al.*, The closing of Tethys and the tectonics of the Himalaya. *Geol. Soc. Am. Bull.*, 1987, **98**, 678–701.
8. Dewey, J. F., Cande, S. C. and Pitman III, W. C., Tectonic evolution of the India/Eurasia collision zone. *Eclogae Geol. Helv.*, 1989, **82**, 717–734.
9. Klootwijk, C. T., Gee, J. S., Peirce, J. W., Smith, G. M. and MacFadden, P. L., An early India–Asia contact, paleomagnetic constraints from Ninetyeast Ridge, ODP Leg 121; with suppl. Data 92-15. *Geology*, 1992, **20**, 395–398.
10. Harrison, T. M., Copeland, P., Kidd, W. S. F. and Yin, A., Raising Tibet. *Science*, 1992, **255**, 1663–1670.
11. Beck, R. A. *et al.*, Stratigraphic evidence for an early collision between northwest India and Asia. *Nature*, 1995, **373**, 55–58.
12. Butler, R., Tectonics – when did India hit Asia? *Nature*, 1995, **373**, 20–21.
13. Rowley, D. B., Age of initiation of collision between India and Eurasia: A review of stratigraphic data. *Earth Planet. Sci. Lett.*, 1996, **145**, 1–13.
14. Yin, A. and Harrison, T. M., Geologic evolution of the Himalayan – Tibetan orogen. *Annu. Rev. Earth Planet. Sci.*, 2000, **28**, 211–280.
15. Najman, Y., Pringle, M., Godin, L. and Oliver, G., Dating of the oldest continental sediments from the Himalayan foreland basin. *Nature*, 2001, **410**, 194–197.
16. Zhu, B., Kidd, W. S. F., Rowley, D. B., Currie, B. S. and Shafique, N., Age of initiation of the India-Asia collision in the east-central Himalaya. *J. Geol.*, 2005, **113**, 265–285.
17. Spears, D. A. and Kanaris-Sotiriou, R., A geochemical and mineralogical investigation of some British and other European tonsteins. *Sedimentology*, 1979, **36**, 407–425.
18. Bohor, B. F. and Triplehorn, D. M., Tonsteins: Altered volcanic–ash layers in coal-bearing sequences. *Geol. Soc. Am. Spec. Pap.*, 1993, **285**, p. 44.
19. Lyons, P. C., Spears, D. A., Outerbridge, W. F., Congdon, R. D., and Evans, Jr. H. T., Euramerican tonsteins: overview, magmatic origin, and depositional-tectonic implications. *Palaeogeogr., Palaeoclimatol., Palaeoecol.*, 1994, **106**, 113–134.
20. Raiverman, V., Stratigraphy and facies distribution, Subathu sediments, Simla Hills, northwestern Himalaya. *Geol. Surv. India, Misc. Publ.*, 1979, **41**, 111–126.
21. Nanda, A. C. and Kumar, K., Excursion guide on the Himalayan Basin (Jammu–Kalakot–Udhampur sector). Wadia Institute of Himalayan Geology, Dehradun, Spl. Publ., 1999, vol. 2, pp. 1–85.
22. Mathur, N. S. and Juyal, K. P., Atlas of early Palaeogene invertebrate fossils of the Himalayan Foothill belt. Wadia Institute of Himalayan Geology, Dehradun, Monogr. 2000, vol. 1, p. 257.
23. Singh, P., The Subathu Group of India. *Geosci. J. Prof. Pap.*, 1980, **1**, 1–92.
24. Kumar, K. and Loyal, R. S., Eocene ichthyofauna from the Subathu Formation, northwestern Himalaya, India. *J. Palaeontol. Soc. India*, 1987, **32**, 60–84.
25. Kumar, K., Srivastava, R. and Sahni, A., Middle Eocene rodents from the Subathu Group, Northwest Himalaya. *Palaeovertebrata France*, 1997, **26**, 83–128.
26. Bhatia, S. B. and Bagi, H., Early Lutetian Charophyta from the Shimla Hills, lesser Himalaya. *Bull. Soc. Bot. France*, 1991, **1**, 7–14.
27. Bhatia, S. B. and Bhargava, O. N., Regional correlation of the Palaeogene sediments of the Himalayan foreland basin. *Palaeontol. Soc. India, Spl. Publ.*, 2005, **2**, 105–123.
28. Sarkar, S. and Singh, H. P., Palynological investigation of Subathu Formation (Eocene) in the Banethi–Bagthan area of H.P., India. *Palaeontogr. Abstr. B*, 1988, **209**, 29–109.
29. Jafar, S. A. and Singh, O. P., K/T boundary species with Early Eocene nannofossils discovered from Subathu Formation, Shimla Himalaya, India. *Curr. Sci.*, 1992, **62**, 409–413.
30. Fisher, R. V. and Schmincke, H. U., *Pyroclastic Rocks*, Springer-Verlag, Berlin, 1984, p. 472.
31. Senkayi, A. L., Dixon, J. B. and Hossner, L. R., Mineralogy and genetic relationships of tonstein, bentonite, and lignitic strata in the Eocene Yegua Formation of east-central Texas. *Clays Clay Miner.*, 1984, **32**, 259–271.
32. Spears, D. A., Kanaris-Sotiriou, R., Riley, N. and Krause, P., Namurian bentonites in the Pennine Basin, UK-Origin and magmatic affinities. *Sedimentology*, 1999, **46**, 385–401.
33. Ece, O. I., Nakagawa, Z.-E. and Schroeder, P. A., Alteration of volcanic rocks and genesis of kaolin deposits in the Sile region, northern Istanbul, Turkey. I: Clay mineralogy. *Clays Clay Miner.*, 2003, **51**, 657–688.
34. Morton, A. C. and Knox, R. W. O'B., Geochemistry of late Palaeocene and early Eocene tephras from the North Sea basin. *J. Geol. Soc. London*, 1990, **147**, 425–437.

35. Taylor, S. R. and McLennan, S. M., *The Continental Crust: Its Composition and Evolution*, Blackwell Sci. Publ., Oxford, 1985, p. 312.
36. Izett, G. A., Volcanic ash beds: Recorders of Upper Cenozoic silicic pyroclastic volcanism in the western United States. *J. Geophys. Res.*, 1981, **86**, 10200–10222.
37. Burger, K., Bandelow, F. K. and Bieg, G., Pyroclastic kaolin coal-tonsteins of the upper carboniferous of Zonguldak and Amasra, Turkey. *Int. J. Coal Geol.*, 2000, **45**, 39–53.
38. Knight, J. A., Burger, K. and Bieg, G., The pyroclastic tonsteins of the Sabero Coalfield, north-western Spain, and their relationship to the stratigraphy and structural geology. *Int. J. Coal Geol.*, 2000, **44**, 187–226.

ACKNOWLEDGEMENTS. We are grateful to Dr B. R. Arora, Director, Wadia Institute of Himalayan Geology, Dehradun for encouragement and providing the necessary facilities to carry out this work. We thank Prof. Ashok Sahni, Panjab University, Chandigarh for inducing enthusiasm in our work on Subathus. Thanks are also due to Dr N. K. Saini, Chandrashekar and N. K. Juyal for XRF and SEM analysis. We thank the anonymous reviewer for useful comments. This work was partly supported by a grant from the Department of Science and Technology, New Delhi.

Received 24 March 2006; revised accepted 26 August 2006